Physics of Plasmas ARTICLE scitation.org/journal/php

Modulation-slippage trade-off in resonant four-wave upconversion

Cite as: Phys. Plasmas **28**, 052112 (2021); doi: 10.1063/5.0046695
Submitted: 5 February 2021 · Accepted: 30 April 2021 ·
Published Online: 20 May 2021

A. Griffith,[a] K. Qu, and N. J. Fisch

AFFILIATIONS

Department of Astrophysical Sciences, Princeton University, Princeton, New Jersey 08540, USA

[a]Author to whom correspondence should be addressed: arbg@princeton.edu

ABSTRACT

Following up on a proposal to use four-wave mixing in an underdense plasma at mildly relativistic laser intensities to produce vastly more energetic x-ray pulses [Malkin and Fisch, Phys. Rev. E **101**, 023211 (2020)], we perform the first numerical simulations in one dimension to illustrate amplification of a short high frequency seed through four-wave mixing. We illustrate how parasitic processes including phase modulation and spatial pulse slippage limit the amplification efficiency. Although the regimes studied were not where the optimal efficiencies were expected, these regimes do expose the basic physical processes at play, while still yielding not insignificant spectral power upshift.

I. INTRODUCTION

Directly producing a megajoule of coherent x rays greatly exceeds the capability of current x-ray technologies such as free electron lasers[1,2] or Compton scattering.[3] An alternative route for producing high-power coherent x rays is through efficient conversion of megajoule ultraviolet pulses, which are available at existing facilities like the National Ignition Facility.[4] However, conventional frequency conversion processes, such as high harmonic generation in gases,[5–7] crystals,[8,9] or relativistic plasma surfaces,[10] cannot scale to the appropriate intensity or efficiency in the x-ray regime.

The challenges of achieving efficient frequency upconversion of high-power lasers can be overcome by working in plasmas. Plasmas can resist the high intensities and high temperatures that disrupt solid or gaseous mediums. Plasmas allow for wave–wave coupling processes, which have been investigated for laser amplification, e.g., Raman scattering,[11–21] Brillioun scattering,[22–27] and magnetized scattering.[28,29] Additionally, four-wave mixing in plasmas using atomic levels for frequency conversion[30] and pondermotive gratings for same frequency amplification[31] have been considered.

In this paper, we consider through numerical simulations the recent proposal to employ four-wave mixing in underdense plasma to achieve both upconversion and amplification.[32] In this proposal, a cascade of nonlinear, resonant four-wave interactions, based on a relativistic nonlinearity, was suggested to achieve up to a megajoule of laser energy in the x-ray regime.[32] In each step of the cascade, two pump waves, at frequencies ω_1 and ω_2, amplify a weak higher frequency seed wave, frequency ω_3. An idler wave at frequency ω_4 is generated to satisfy the resonance conditions,

$$\omega_j^2 = \omega_{pe}^2 + c^2 k_j^2, \quad \omega_{pe}^2 = \frac{4\pi n_e e^2}{m_e}, \tag{1}$$

$$\omega_1 + \omega_2 = \omega_3 + \omega_4, \tag{2}$$

$$\mathbf{k_1} + \mathbf{k_2} = \mathbf{k_3} + \mathbf{k_4}. \tag{3}$$

Here, the wave frequency ω_j corresponds to wavevector k_j ($j = 1, 2, 3, 4$) and plasma frequency ω_{pe}, for an unperturbed electron fluid with particle charge e, mass m_e, and density n_e. As the idler frequency may be small, the seed frequency for each iteration can reach up to the sum of the two pump frequencies. Each interaction can thus give a multiplicative, rather than additive, change in frequency. With iterated interactions, it might be possible to step up orders of magnitude in frequency. It is the aim of this work to simulate one step of this cascade.

Ideally, the four-wave mixing can increase frequency with up to unity efficiency. The maximum efficiency is achieved when the pumps are completely consumed. If the symmetric pumps are ever depleted simultaneously, the four-wave interaction terminates. For synchronously depleted pumps all the wave energy is in the seed and the idler, and the pumps cannot regrow. Thus, the energy could, in principle, flow from the pumps to the seed and idler and never flow back to the pumps. If the idler frequency is sufficiently low, it carries away negligible energy, resulting in almost all energy being consumed by the seed. The unidirectional energy transfer possible in the four-wave mixing

process[32] represents a significant advantage compared to three-wave scattering processes, which are susceptible to pump reamplification.

However, the elegant resonant four-wave interaction becomes complicated when taking into account phase modulation. Phase modulation changes the wave frequencies asynchronously with amplitude, thereby pushing the interaction out of resonance. The same nonlinearity in the transverse direction can also result in filamentation of the pumps or seed. To counteract the problems arising from phase modulation, the initial proposal suggested using a second signal and idler pair, namely a dual-seed approach, to balance the self- and cross-beam phase modulation terms against each other.[32]

In this paper, using numerical simulations, we first confirm the ideal case, namely that, absent modulation, seed pulse amplification indeed occurs through four-wave mixing, with the amplified pulse advantageously appearing as a single humped output pulse. Next, we show how the efficiency is limited by phase modulation, although significant power is still transferred to higher frequencies. The four-wave mixing process is additionally complicated by variable group velocities and dynamic envelope amplitudes. Next for illustrative purposes, we considered a six-wave configuration to reduce the phase modulation around a set operating point. The six-wave case considered is chosen, in part, for its ease in simulation and for direct comparison to the four-wave cases. It does not take full advantage of the dual-seed approach which requires a more controlled arrangement. Although significant energy transfer still occurs in the non-optimal six-wave case, better performance is achieved, at least for the cases considered here, with a single seed with the four-wave parameters selected to minimize phase modulation. However, the six-wave case, in exhibiting not insignificant energy transfer to higher frequencies, despite the conditions being less than optimal, does expose both the upside potential and the key physical issues in realizing multi-wave upconversion in underdense plasma.

II. RESONANCE CONDITIONS

The resonance conditions, Eqs. (2) and (3), determine the frequencies and propagation velocities of the four waves. Four parallel waves are not desirable because they yield only two sets of trivial solutions: either $\omega_1 = \omega_3$ corresponding to no frequency upconversion, or $\omega_{pe} = 0$ corresponding to no four-wave coupling. Both solutions defeat the purpose of laser frequency upconversion. Satisfying Eqs. (2) and (3) while achieving frequency upconversion with a finite coupling coefficient requires misalignment. Here, we note that frequency upconversion with colinear laser wavevectors is indeed possible when additionally manipulating the phase modulation,[33] but this approach is beyond the scope of our current paper.

The valid seed wavevectors, $\mathbf{k_3} = (k_{3_\parallel}, k_{3_\perp})$, form an ellipse determined by the pump wavevectors, $\mathbf{k_1} = (k_{1_\parallel}, k_{1_\perp})$ and $\mathbf{k_2} = (k_{2_\parallel}, k_{2_\perp})$. For convenience, we rotate the frame such that $k_{1_\perp} = -k_{2_\perp}$, and define quantities $2k = |\mathbf{k_1} + \mathbf{k_2}| = k_{1_\parallel} + k_{2_\parallel}$ and $2\omega = \omega_1 + \omega_2$,

$$1 - \frac{\omega_{pe}^2}{\omega^2 - c^2k^2} = \frac{c^2(k_{3_\parallel} - k)^2}{\omega^2} + \frac{c^2k_{3_\perp}^2}{\omega^2 - c^2k^2}. \tag{4}$$

The ellipse, as illustrated in Fig. 1, represents the complete set of pump–pump and signal–idler wavevector pairs. It has two foci, located at

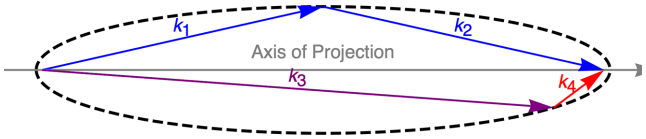

FIG. 1. The dashed ellipse defines the resonance condition, setting the possible wavevector pairs, (1, 2) and (3, 4). Simulations in one dimension are projected onto a single axis (gray) along the midline of the ellipse.

$$k\left(1 \pm \sqrt{1 - \frac{\omega_{pe}^2}{\omega^2 - c^2k^2}}\right). \tag{5}$$

The seed frequency is maximized when $\mathbf{k_3}$ extends beyond the right focus and touches the rightmost point on the ellipse, i.e.,

$$\max|\mathbf{k_3}| = k + c^{-1}\omega\sqrt{1 - \frac{\omega_{pe}^2}{\omega^2 - c^2k^2}}. \tag{6}$$

For fixed pump frequencies, the maximum seed frequency is achieved when the pumps are misaligned by an angle

$$\theta_{1,2} \approx \sqrt{(c|\mathbf{k_1}||\mathbf{k_2}|)^{-1}(|\mathbf{k_1}| + |\mathbf{k_2}|)\omega_{pe}}. \tag{7}$$

Note that, in depicting the ellipse in Fig. 1, in contrast to the limiting case portrayed in previous work,[32] all wavevectors are not necessarily chords on the ellipse. The wavevectors only approach chords in the high frequency paraxial limit when both $\omega_{pe}^2/(\omega^2 - c^2k^2)$ and $1 - \omega^{-2}c^2k^2$ vanish simultaneously. In this limit, the ellipse becomes long and thin, and approaches a line segment between the foci at 0 and $2k$. Depending on the magnitude of the plasma frequency and the angle between the pumps, the origin and end point of the $\mathbf{k_1}$ and $\mathbf{k_2}$ or $\mathbf{k_3}$ and $\mathbf{k_4}$ pairs may lie inside or outside the ellipse.

The required wavevector misalignment results in slippage between the four waves. The angles, and consequently velocities, between the rest of the wavevectors are best interpreted through considering Fig. 1. As ω_3 increases, it pulls the tip of $\mathbf{k_3}$ toward the rightmost point of the ellipse, becoming more parallel with the major axis. To satisfy the resonance conditions, $\mathbf{k_4} = (k_{4_\parallel}, k_{4_\perp})$ must correspondingly tilt more inward. There is a resulting ordering of $|k_{4_\perp}/k_{4_\parallel}| > |k_{1,2_\perp}/k_{1,2_\parallel}| > |k_{3_\perp}/k_{3_\parallel}|$. In the projection, the misalignment drives $v_{3_\parallel} > v_{1,2_\parallel} > v_{4_\parallel}$, causing a slippage between the waves for $v_{j_\parallel} = c^2k_{j_\parallel}/\omega_j$.

The slippage can be reduced with smaller pump laser angles, but plasma dispersion must increase to keep the four-wave coupling rate constant. The four-wave coupling rate,[32] γ, scales with both the angle between the pump beams and the plasma frequency, i.e.,

$$\gamma \approx \frac{3}{2}\frac{k_{1,2_\perp}^2\omega_{pe}^2}{k_{1,2}^2\sqrt{\omega_3\omega_4}}\left|\frac{eA_{1,2}}{m_ec^2}\right|^2. \tag{8}$$

Decreasing misalignment and dispersion both reduce the four-wave coupling through $k_{1,2_\perp}/k_{1,2}$ and $\omega_{pe}^2/\sqrt{\omega_3\omega_4}$, respectively. A decrease in either term may be compensated for through increasing the magnitude of the pump vector potential, $A_{1,2}$. But the compensation is capped as pump strength may only grow as long as $|eA_{1,2}| \ll m_ec^2$ to remain in the mildly relativistic regime. The

perpendicular wavevector component and dispersion contribute similarly to the parallel velocity,

$$v_{j_\parallel}/c \approx 1 - k_{j_\perp}^2 k_j^{-2} - \omega_{pe}^2 (2c^2 k_j^2)^{-1}. \tag{9}$$

Either misalignment, $k_{j_\perp}^2 k_j^{-2}$, or dispersion, $\omega_{pe}^2 (2c^2 k_j^2)^{-1}$, may be small, but not both if strong coupling is desired.

The misalignment is the dominant effect for large upconversion. For large upconversion, $k_{1,2_\perp} \approx k_{1,2}\theta_{1,2}/2$. With $\theta_{1,2}$ chosen in accordance with Eq. (7), the misalignment term contributes slippage linear in $\omega_{pe}/ck_{1,2}$. The misalignment slippage term which is linear in ω_{pe} dominates the dispersion term which is quadratic in ω_{pe} as the waves remain in the underdense regime. The slippage due to differences in misalignment can be demonstrated to have a significant effect on the four-wave upconversion process.

III. FOUR-WAVE MODEL

The four-wave interaction is governed by a set of nonlinear wave equations derived through combining Maxwell's equations, the relativistic equations of motion for a constant density mono-energetic electron fluid, and the neutralizing effect of a static ion background. Each wave has a scaled complex envelope $b_j = \sqrt{\omega_j} eA_j/(m_e c^2)$, where A_j is the vector potential amplitude for wave j. All the waves are polarized perpendicular to the plane in which all $\mathbf{k_j}$ are chosen to lie. The four-wave interaction originates from the lowest order relativistic correction to the electron equations of motion, expanding in $eA_j/(m_e c^2)$.

To pose the problem in 1D (one dimension), the dynamical equations[32] are projected onto the dominant axis of propagation. The axis, denoted x, lies on the center of the ellipse governed by Eq. (4), chosen such that $k_{\perp_j}/k_{\parallel_j} \ll 1$ for all waves. The resulting dynamical equations contain longitudinal propagation and the lowest order relativistic correction,

$$i(\partial_t + c^2 k_{j_x} \omega_j^{-1} \partial_x) b_j = \delta\omega_j b_j + \partial_{b_j^*} \mathscr{H}, \tag{10}$$

$$\delta\omega_j = \frac{\omega_{pe}^2}{2\omega_j} \sum_{l=1}^{4} \frac{|b_l|^2}{\omega_l} \times \begin{cases} f_{+,j,l} + f_{-,j,l} - 1, & j \neq l, \\ f_{+,j,l} - 1, & j = l, \end{cases} \tag{11}$$

$$\mathscr{H} = V_{1,2,3,4} b_1 b_2 b_3^* b_4^* + c.c., \tag{12}$$

$$V_{j,l,m,n} = \frac{\omega_{pe}^2 (f_{+,j,l} + f_{-,j,n} + f_{-,l,n})}{2\sqrt{\omega_j \omega_k \omega_m \omega_n}}, \tag{13}$$

$$f_{\pm,j,l} = \frac{c^2 (\mathbf{k_j} \pm \mathbf{k_l})^2}{(\omega_j \pm \omega_l)^2 - \omega_{pe}^2} - 1. \tag{14}$$

The LHS of Eq. (10) describes the wave propagation in the x direction at group velocity $v_j = c^2 k_{j_\parallel} \omega_j^{-1}$. The RHS consists of a modulational term, $\delta\omega_j$, which results in amplitude dependent frequency shifts, and a four-wave coupling term, captured through the Hamiltonian $\mathscr{H}$.

The paraxial equations (10) are evolved numerically to capture the long time amplification of the seed. We conduct the simulations in a frame moving with the seed to reduce the computational domain. The two pump waves are initialized evenly out in front of the signal seed, and the seed runs through the waves picking up their energy. The fourth idler wave, which has the smallest parallel group velocity, quickly flows out of the left side of the domain. The equations are evolved using Dedalus, a general spectral PDE solver.[34]

IV. IDEAL FOUR-WAVE BEHAVIOR

To illustrate the opportunities in four-wave resonant mixing, we first simulate an ideal scenario for the four-wave interaction. In this simulation, phase modulation is assumed to be negligible, which will expose the successes and challenges intrinsic to four-wave resonant coupling. Consider then pumps that have the same frequency, but with equal and opposite $k_\perp$. The resulting synchronous pumps amplify the seed, which grows monotonically in energy.

Figure 2 shows three snapshots of a seed being amplified such that the final energy $E_{\text{final}} = 78E_0$. The first snapshot shows the initial conditions (held constant across all simulations). The pumps are just beginning to intersect with the seed and initiate the linear stage of amplification. When the pumps are still strong, amplification occurs widely, resulting in the long seed tail shown in the second snapshot. As the seed strength grows the pumps become depleted, and amplification occurs closer to the front of the seed. For a sufficiently strong seed, all of the pump energy is consumed at the seed's leading edge. The signal then grows continually steeper in time, taking long duration pump energy and compressing it into a shorter peak. The compression of pump energy is similar to that in Raman amplification.[11] Like Raman amplification, some energy is lost to a disposable wave, the fourth wave here, or the plasma wave in the case of Raman amplification. But, unlike Raman amplification, all energy could ideally be deposited into a single growing peak, without producing the amplified pulse train characteristic of the π pulse solution for resonant three-wave interactions.[11]

Thus, considerable upshift and efficiency are easily achieved in the idealized four-wave resonant interaction. The results shown in Fig. 2 achieve a 40% increase in pump photon energy with $\omega_1 + \omega_2 \sim 10^2 \omega_{pe}$. When pump depletion is achieved, the energy conversion efficiency may become as high as 70%, with the remaining energy

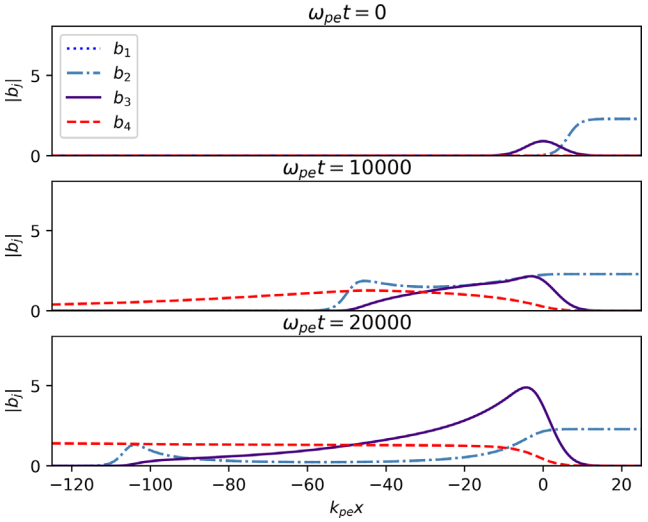

FIG. 2. Numerical snapshots of normalized magnitude b_j with upconversion factor $\omega_3/\omega_{1,2} = 1.4$. Snapshots are shown at $\omega_{pe}t = 0$, 10^4, 2×10^4 with $\delta\omega_j$ set to 0. Pumps (b_1, dotted, and b_2, dot-dashed) are fed in with relativistic factor $|a_{1,2}| = 0.33$, with the seed initialized with relativistic factor $|a_3| = 0.11$. Resonance conditions are $\omega_1 = \omega_2 = 47\omega_{pe}$ and $\omega_3 = 66\omega_{pe}$.

flowing to the idler wave. The frequency-upshifted output wave is advantageously single-peaked.

A larger seed frequency corresponds to a higher limiting efficiency, but, in practice, this higher efficiency is difficult to achieve within a finite plasma length. At higher seed frequency, upconversion is hampered by the consequent decrease in the coupling coefficient. Figure 3 shows the reduction in the realized amplification efficiency with increasing seed frequency. Weaker coupling increases the time to reach the pump depletion regime. Only at pump depletion is maximum efficiency and steepening achieved. For a limited interaction region, the maximum efficiency may never be reached, and upconversion may be strictly worse for higher frequencies.

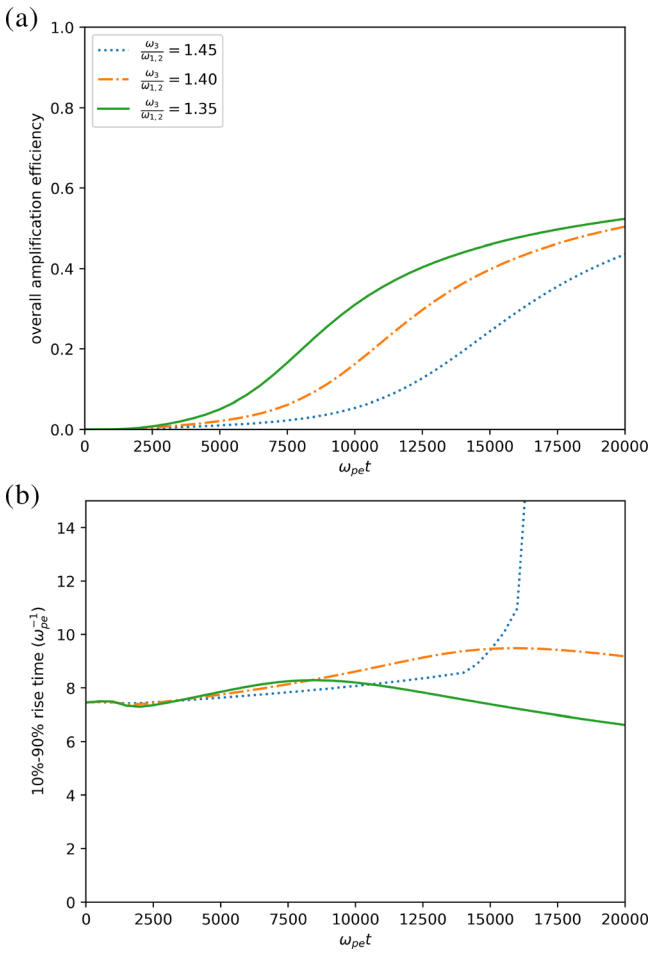

FIG. 3. Increasing $\omega_3/\omega_{1,2}$ decreases coupling, resulting in a longer time to efficiency saturation and steepening of the leading edge. Over a finite timescale, this reduces efficiency, even though higher saturation efficiency may be reached. With low enough coupling, amplification may occur behind the seed pulse, leading to a discrete second peak, and a corresponding jump in rise time. $\omega_3 = 1.4\omega_{1,2}$ corresponds with evolution shown in Fig. 2. All efficiencies are simulation with Fig. 2 parameters, varying ω_3. $\omega_3 = 1.35, 1.40, 1.45\omega_{1,2}$ correspond to ideal efficiencies of 67.5, 70.0, 72.5%, respectively. Efficiency in all plots is calculated as total change in seed energy divided by the total pump energy which has flowed into the domain.

Slower amplification also results in a lower contrast pulse, as shown in Fig. 3. With lower coupling, the peak takes longer to shift forward. Low enough coupling can result in a second peak, resulting in a discrete increase in the rise time. A low ratio of $\omega_3/\omega_{1,2}$ is thus more advantageous in maintaining a steep leading edge.

V. PHASE MODULATION AND THE FOUR-WAVE INTERACTION

The ideal solution, however, neglected phase modulation. The phase modulation terms must in fact be included to capture fully the lowest order relativistic behavior. These terms can push the four-wave interaction out of resonance. For example, the issue caused by phase modulation can be seen in the case of the exact same wavevectors used in the ideal regime, e.g., Fig. 2. The same frequency pumps cancel in the denominator in Eq. (14), making phase modulation scale $\propto c^2k_{1_\perp}^2\omega_{pe}^{-2}$. A large value of $ck_{1_\perp}\omega_{pe}^{-1}$ is required for significant four-wave coupling, resulting in extreme phase modulation. For the parameters used in Fig. 2, the strength of this term results in a perturbation from resonance that makes amplification untenable, with $\delta\omega_{1,2}$ approximately 40 times the seed growth rate. Furthermore, the extreme amplitude dependent phase modulation rapidly distorts the pumps. The wavevectors must then change for the interaction to coherently amplify the seed.

The resonance drift caused by phase modulation can be reduced through pump detuning. Pump detuning reduces the strength of the $f_{-,1,2}$ term to $\propto c^2k_{1_\perp}^2(\omega_1-\omega_2)^{-2} \ll c^2k_{1_\perp}^2\omega_{pe}^{-2}$ for $\omega_1-\omega_2 \gg \omega_{pe}$. But detuning the pumps, while necessary to reduce modulation, has a corresponding cost in pump–pump slippage. The frequency detuned pumps have different velocities relative to the seed, so that they no longer move in perfect unison. As a result, the perfectly simultaneous pump depletion of the ideal case is no longer possible. To isolate the indirect effects, namely slippage, from the direct effects, namely phase modulation, we performed simulations with the same detuned pumps, both excluding and including the $\delta\omega$ term. Excluding the $\delta\omega_j$ term, asynchronous pumps can cause the four-wave interaction to work in reverse, leading to re-amplified pumps and reduced energy conversion efficiency, illustrated by Fig. 4. In Fig. 5, phase modulation is added into the same simulation. The phase modulation becomes significant at high seed amplitude, pushing the waves out of resonance and further lowering amplification.

The combination of detuning and phase modulation apparently sets a lower achievable maximum efficiency. The efficiency evolution of the detuned simulations with and without phase modulation both perform worse than the earlier ideal simulations, shown in Fig. 6. The efficiency rises faster in the detuned simulations, as detuning moderately increases coupling. However, it becomes bounded at a lower level from detuning, and is driven even lower from phase modulation. Both factors contribute significantly, with slippage on its own driving a large change in efficiency. The importance of slippage as an indirect effect will persist even as we attempt to mitigate the modulation through other means.

VI. COUNTERBALANCING PHASE MODULATION

There was an interesting suggestion on how to reduce the detrimental effects of modulation, namely by adding two more waves to the four-wave approach.[32] The additional beams induce cross-beam modulation which could, in principle, counterbalance against the pump/pump phase modulation. Cross-beam phase modulation

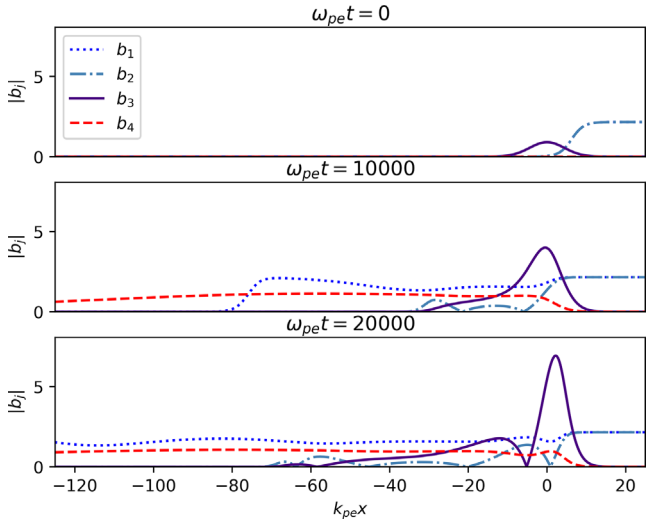

FIG. 4. Numerical snapshots of normalized magnitude b_j at $\omega_{pe}t = 0$, 10^4, 2×10^4 for $2\omega_3/(\omega_1 + \omega_2) = 1.4$ with $\delta\omega_j$ set to 0, but with pumps detuned such that $\omega_2 - \omega_1 = 11\omega_{pe}$. Pumps are initialized with $|a_1| = 0.33$ and seed with amplitude $|a_3| = 0.11$. Resonance conditions are $\omega_1 = 42\omega_{pe}$, $\omega_2 = 52\omega_{pe}$, and $\omega_3 = 66\omega_{pe}$.

between slightly detuned seeds can oppose the cross-beam phase modulation between the slightly detuned pumps. Generally, this could be used to maintain the resonance across a wide range of pump and seed parameters. Here we describe the approach of using two seeds to reduce phase modulation. In Sec. VII we adapt the matched seeds to improve the phase modulation around a single point of perfect

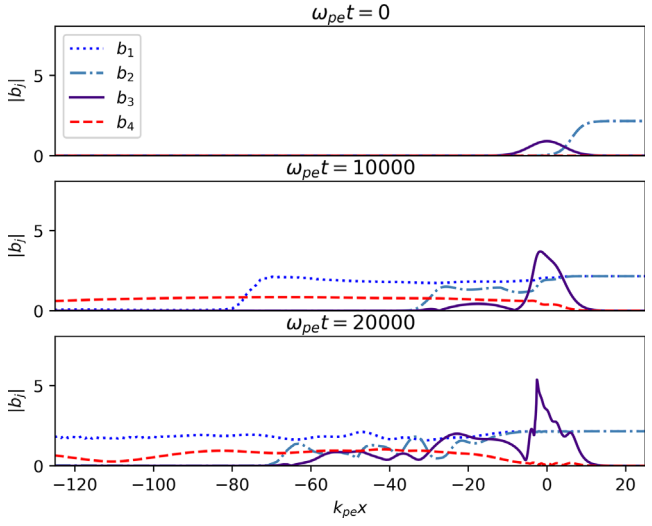

FIG. 5. Numerical snapshots of normalized magnitude b_j at $\omega_{pe}t = 0$, 10^4, 2×10^4 for $2\omega_3/(\omega_1 + \omega_2) = 1.4$ with $\delta\omega_j$ governed by Eq. (11), but with pumps detuned such that $\omega_2 - \omega_1 = 11\omega_{pe}$. Pumps are initialized with $|a_1| = 0.33$ and seed with amplitude $|a_3| = 0.11$. Resonance conditions are $\omega_1 = 42\omega_{pe}$, $\omega_2 = 52\omega_{pe}$, and $\omega_3 = 66\omega_{pe}$.

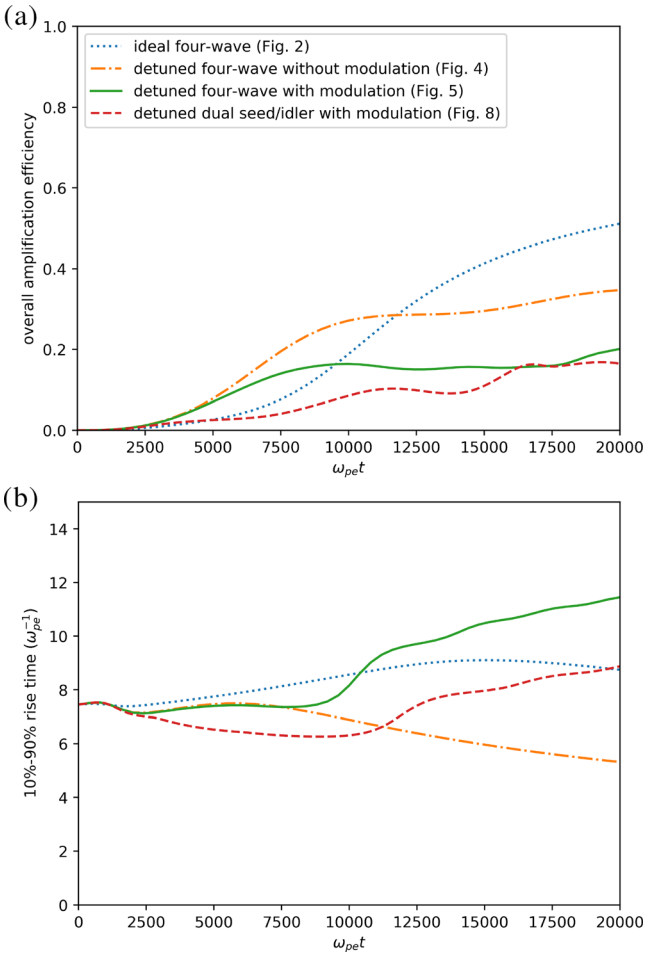

FIG. 6. Efficiency and rise time evolution corresponding to snapshots presented in Figs. 2, 4, 5, and 8. Symmetric pumps equilibrate at a much longer timescale, but at higher level compared to non-ideal alternatives. The higher coupling from detuned pumps results in more leading edge steepening, but when phase modulation is included this steepening is limited and eventually reversed. All cases correspond with $2\omega_3/(\omega_1 + \omega_2) = 1.4$.

resonance as a comparable case against the simulations described in Sec. V. The full dual-seed concept allows for a wider range of manipulation of pump and seed properties which we do not consider here.

Two additional waves obey the same resonance conditions [Eqs. (15) and (16)], where wave 5 will be the second seeded signal and a wave 6 will be the second idler,

$$\omega_1 + \omega_2 = \omega_3 + \omega_4 = \omega_5 + \omega_6, \tag{15}$$

$$\mathbf{k_1} + \mathbf{k_2} = \mathbf{k_3} + \mathbf{k_4} = \mathbf{k_5} + \mathbf{k_6}. \tag{16}$$

The dynamical equations must be adjusted to account for the two new waves. Evolving two additional waves adds additional phase modulation terms,

$$\delta\omega_j = \frac{\omega_{pe}^2}{2\omega_j} \sum_{l=1}^{6} \frac{|b_l|^2}{\omega_l} \times \begin{cases} f_{+,j,l} + f_{-,j,l} - 1 & l \neq j, \\ f_{+,j,l} - 1 & l = j. \end{cases} \tag{17}$$

The phase modulation has been extended to all six waves, with the novelty primarily contained in the strength of the new $f_{-,3,5}$ term. The similarly large $f_{-,4,6}$ does not significantly contribute as waves 4 and 6 never grow large, slipping behind the point of interaction much faster than signal and pump waves.

The Hamiltonian governing the four-wave coupling must also be extended to accommodate waves 5 and 6,

$$\mathscr{H} = V_{1,2,3,4} b_1 b_2 b_3^* b_4^* + V_{1,2,5,6} b_1 b_2 b_5^* b_6^* + V_{3,4,5,6} b_3 b_4 b_5^* b_6^* + c.c. \quad (18)$$

A second set of four-wave coupling results in symmetric pump–pump to signal–idler transfer for waves five and six, $V_{1,2,5,6}$, as previously only was for waves three and four, $V_{1,2,3,4}$. The resonance conditions imply a novel term which is the signal–idler to dual signal–dual idler coupling, $V_{3,4,5,6}$. When both the 3, 5 and 4, 6 pairs are perfectly symmetric, the additional coupling should not change the four-wave behavior, but when the signal waves begin to slip, the coupling can push energy between the desynchronized seeds.

The new phase modulation terms may be arranged, with specific finite wave amplitudes, such that the four waves are in perfect resonance. The arrangement is accomplished through changing the detuning between the two seeds. Changing the detuning alters the seed to pump ratio at which all phase modulation terms balance. Two cases with $\omega_3 - \omega_5 = 2.5\omega_{pe}$, and $5\omega_{pe}$ are compared to the unaltered scheme in Fig. 7. Weak detuning results in extreme sensitivity of the resonance to the seed to pump ratio and a low relative seed strength at which the terms balance. Larger detuning results in lower sensitivity, and counterbalancing at larger seed amplitude, where the counterbalancing is needed most. Of course, the perfect resonance may be lost as the waves evolve in time away from the arranged amplitudes.

VII. SHORT PULSES WITH MULTIPLE SEEDS

We consider a simple six-wave process in which the phasing is balanced at a single ratio of seed to pump amplitude. While not taking advantage of the full range of six-wave possibilities, phase modulation can be reduced throughout the amplification process. Phase modulation should now track the $\omega_3 - \omega_5 = 5\omega_{pe}$ line shown in Fig. 7 rather than the more strongly detuned four-wave scenario presented in the same figure. While not employing the dual-seed approach, which requires a more elaborate arrangement to balance the phasing for all time, this example serves well for illustrative purposes, since it can be compared directly to the four-wave case considered above.

Thus, a fifth and sixth wave are added to the previous simulations, obeying Eqs. (15) and (16). The new initial conditions are shown in the first snapshot of Fig. 8. Now, the second signal seed is given the same initial envelope as the initial signal, such that initially waves three and five completely overlap. Wave five is detuned from wave three by $5\omega_{pe}$, and slips behind the leading seed as can be seen in the second snapshot. Finite detuning results in group velocity differences, and the new lower frequency second signal wave falls behind on a faster timescale than the amplification. The leading signal wave then gains more energy than the second signal. The signal-to-signal coupling further amplifies this issue as it drives an energy transfer between the two signal waves. The required symmetry between the two signal waves quickly fades, and the simulation begins to converge toward the earlier unaltered simulation, where the last snapshots of Figs. 8 and 5 have similar signal wave envelopes.

As with detuning the pumps, there is apparently an unavoidable trade-off between reducing phase modulation and slippage. The phase modulation dominantly affects the resonance through the seed–seed coupling, $f_{-,3,5}$. The sensitivity of the resonance to the seed strength scales inversely with the detuning,

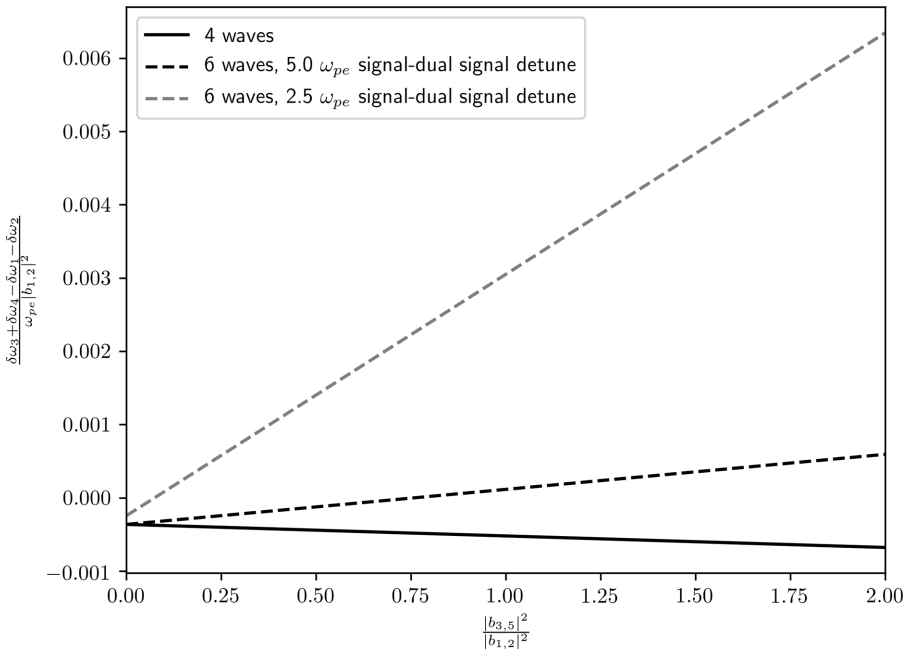

FIG. 7. Resonance detuning, $\delta\omega_1 + \delta\omega_2 - \delta\omega_3 - \delta\omega_4$, may have a different sign dependence on seed strength if the dual seed approach is used. A point of perfect resonance is achieved at finite signal and pump amplitude with appropriate application of the dual seed strategy.

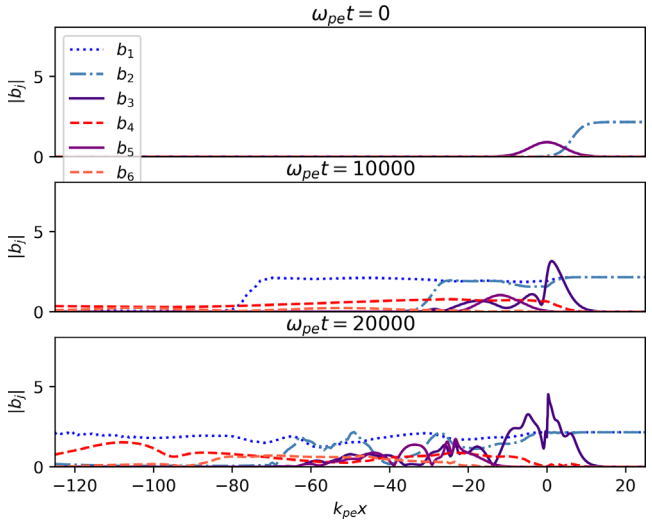

FIG. 8. Numerical snapshots of normalized magnitude b_j at $\omega_{pe}t = 0$, 10^4, 2×10^4 for $2\omega_3/(\omega_1 + \omega_2) = 1.4$ with $\omega_2 - \omega_1 = 11\omega_{pe}$ and with a second seed and idler such that $\omega_3 - \omega_5 = 5\omega_{pe}$. Pumps are initialized with $|a_1| = 0.33$ and the seed is given amplitude $|a_3| = 0.11$. Resonance conditions are $\omega_1 = 42\omega_{pe}$, $\omega_2 = 52\omega_{pe}$, $\omega_3 = 66\omega_{pe}$, and $\omega_5 = 61\omega_{pe}$.

$$\frac{\partial(\delta\omega_1 + \delta\omega_2 - \delta\omega_3 - \delta\omega_4)}{\partial(|b_{3,5}|^2)} \sim \frac{2c^2k_{3_\perp}^2\omega_{pe}^2}{\omega_3^2(\omega_3 - \omega_5)^2}. \tag{19}$$

While the sensitivity of the resonance decreases with larger seed–seed detuning, the slippage between the two waves increases linearly,

$$v_{3_\parallel} - v_{5_\parallel} \sim \frac{2c^3(\omega_3 - \omega_5)k_{3_\perp}^2}{\omega_3^3}. \tag{20}$$

Both low sensitivity and low slippage cannot be achieved simultaneously, but both are needed to make the six-wave approach effective.

The simplified six-wave strategy apparently does not improve on the four-wave strategy. This is not completely surprising, as we have applied the approach to a different regime than what was originally proposed. The lack of improvement is seen not only in pulse structure, in Fig. 8, but also in the efficiency, as shown in Fig. 6. Only after the second seed has fully fallen behind the original seed does the efficiency begin to approach that of the four-wave approach. While this simplified six-wave approach does not improve upon the comparable simpler four-wave approach, the comparison between the two does expose the physical processes. Also, even under these less than optimal conditions, there remains significant energy transfer to higher frequencies, even if this transfer does not approach yet the theoretically possible almost unity efficiency.

VIII. CONCLUSIONS

In conclusion, we described, using one-dimensional simulations, how idealized four-wave mixing with two balanced pumps can amplify, with high efficiency, significantly upshifted pulses. However, this idealized case neglected phase modulation terms, which are difficult to cancel out. When phase modulation is considered, the pump wavevectors must be changed to reduce cross-beam phase modulation. With just a simple strategy to mitigate phase modulation, successful upconversion can be achieved. Although the efficiency is significantly lower than the almost perfect efficiency in the ideal scenario, significant power can still be upconverted to higher frequency.

To illustrate the physics at play when other means are used to mitigate the phase modulation, a simplified six-wave strategy was employed by adding a second signal–idler pair of pulses. Although the perturbation from resonance could be reduced, this strategy did not improve the efficiencies. The second seed's slippage resulted in asymmetry between seeds, which was further exacerbated by additional coupling. The asymmetry between the seeds apparently served more to reduce the amplification than to remove the limiting effects of phase modulation. Thus, optimizing for low slippage was seen to be as important as optimizing for favorable four-wave coupling and phase modulation mitigation.

To be maximally efficient, experimental implementation of four-wave upconversion must thus first overcome constraints set by slippage. While longitudinal slippage affects the four-wave process, transverse slippage requires wide pulses for overlap to be maintained over the duration of the interaction. For the parameters considered here ($|a_1| = 0.33$, $k_{1_\perp}/|\mathbf{k_1}| = 0.14$, $\omega_1 = 47\omega_{pe}$), 350 nm pump pulses would travel 5.2 cm and slip transversely 7 mm over the duration. Experiments with 350 nm wavelength pumps corresponding to the simulations described here would have pump and seed intensities of 1.2×10^{18} and 2.3×10^{17} W/cm^2, respectively, implying pump powers in the hundreds of petawatts for 7 mm beamwidths, well beyond current capabilities. Limits on the perpendicular wavevector components also limit the achievable upconversion and efficiency, both posing issues if iterated many times to achieve high frequencies. An implementation that will deliver significant energy to the x-ray regime will need to overcome these factors.

Some of these issues result from the simple implementation considered here. Previous work has addressed how these problems could be overcome, including difficulties arising from slippage, for example by a more complicated arrangement of multiple pulses using the dual seed approach or arranging for grazing angle reflections in a channel.[32] Another approach is to arrange for carefully chosen colinear pulses.[33]

The numerical simulations presented here are thus just a first cut at illustrating the issues in optimizing the recently proposed four-wave coupling in underdense plasma to produce frequency upshifted laser power with very high efficiency. While the theoretically maximum achievable efficiencies were far from reached, the non-optimal simple cases here showed decent efficiency with significant energy transfer. Moreover, the possibilities explored here do not exhaust what might be attempted to achieve those theoretically achievable efficiencies. Although enlarging the parameter space introduces promising possibilities, these possibilities do come with added complexity in experimental realization and computational cost in simulations. However, what we did explore already illustrated both the very promising potential of the four-wave upconversion effect and the issues that must be confronted in realizing it.

ACKNOWLEDGMENTS

The work is supported by NNSA Grant No. DE-NA0003871.

DATA AVAILABILITY

The data that support the findings of this study are available from the corresponding author upon reasonable request.

REFERENCES

[1]P. Emma, R. Akre, J. Arthur, R. Bionta, C. Bostedt, J. Bozek, A. Brachmann, P. Bucksbaum, R. Coffee, F.-J. Decker, Y. Ding, D. Dowell, S. Edstrom, A. Fisher, J. Frisch, S. Gilevich, J. Hastings, G. Hays, P. Hering, Z. Huang, R. Iverson, H. Loos, M. Messerschmidt, A. Miahnahri, S. Moeller, H.-D. Nuhn, G. Pile, D. Ratner, J. Rzepiela, D. Schultz, T. Smith, P. Stefan, H. Tompkins, J. Turner, J. Welch, W. White, J. Wu, G. Yocky, and J. Galayda, "First lasing and operation of an Ångstrom-wavelength free-electron laser," Nat. Photonics **4**, 641–647 (2010).

[2]C. Pellegrini, A. Marinelli, and S. Reiche, "The physics of x-ray free-electron lasers," Rev. Mod. Phys. **88**, 015006 (2016).

[3]N. D. Powers, I. Ghebregziabher, G. Golovin, C. Liu, S. Chen, S. Banerjee, J. Zhang, and D. P. Umstadter, "Quasi-monoenergetic and tunable X-rays from a laser-driven Compton light source," Nat. Photonics **8**, 28–31 (2014).

[4]C. A. Haynam, P. J. Wegner, J. M. Auerbach, M. W. Bowers, S. N. Dixit, G. V. Erbert, G. M. Heestand, M. A. Henesian, M. R. Hermann, K. S. Jancaitis, K. R. Manes, C. D. Marshall, N. C. Mehta, J. Menapace, E. Moses, J. R. Murray, M. C. Nostrand, C. D. Orth, R. Patterson, R. A. Sacks, M. J. Shaw, M. Spaeth, S. B. Sutton, W. H. Williams, C. C. Widmayer, R. K. White, S. T. Yang, and B. M. V. Wonterghem, "National Ignition Facility laser performance status," Appl. Opt. **46**, 3276–3303 (2007).

[5]M. Ferray, A. L'Huillier, X. F. Li, L. A. Lompre, G. Mainfray, and C. Manus, "Multiple-harmonic conversion of 1064 nm radiation in rare gases," J. Phys. B **21**, L31–L35 (1988).

[6]F. Krausz and M. Ivanov, "Attosecond physics," Rev. Mod. Phys. **81**, 163–234 (2009).

[7]T. Popmintchev, M.-C. Chen, D. Popmintchev, P. Arpin, S. Brown, S. Ališauskas, G. Andriukaitis, T. Balčiunas, O. D. Mücke, A. Pugzlys, A. Baltuška, B. Shim, S. E. Schrauth, A. Gaeta, C. Hernández-García, L. Plaja, A. Becker, A. Jaron-Becker, M. M. Murnane, and H. C. Kapteyn, "Bright coherent ultrahigh harmonics in the keV X-ray regime from mid-infrared femtosecond lasers," Science **336**, 1287–1291 (2012).

[8]S. Ghimire, A. D. DiChiara, E. Sistrunk, P. Agostini, L. F. DiMauro, and D. A. Reis, "Observation of high-order harmonic generation in a bulk crystal," Nat. Phys. **7**, 138–141 (2011).

[9]S. Ghimire and D. A. Reis, "High-harmonic generation from solids," Nat. Phys. **15**, 10–16 (2019).

[10]U. Teubner and P. Gibbon, "High-order harmonics from laser-irradiated plasma surfaces," Rev. Mod. Phys. **81**, 445–479 (2009).

[11]V. M. Malkin, G. Shvets, and N. J. Fisch, "Fast compression of laser beams to highly overcritical powers," Phys. Rev. Lett. **82**, 4448–4451 (1999).

[12]Y. Ping, W. Cheng, S. Suckewer, D. S. Clark, and N. J. Fisch, "Amplification of ultrashort laser pulses by a resonant Raman scheme in a gas-jet plasma," Phys. Rev. Lett. **92**, 175007 (2004).

[13]J. Ren, S. Li, A. Morozov, S. Suckewer, N. A. Yampolsky, V. M. Malkin, and N. J. Fisch, "A compact double-pass Raman backscattering amplifier/compressor," Phys. Plasmas **15**, 056702 (2008).

[14]C.-H. Pai, M.-W. Lin, L.-C. Ha, S.-T. Huang, Y.-C. Tsou, H.-H. Chu, J.-Y. Lin, J. Wang, and S.-Y. Chen, "Backward Raman amplification in a plasma waveguide," Phys. Rev. Lett. **101**, 065005 (2008).

[15]Y. Ping, R. K. Kirkwood, T.-L. Wang, D. S. Clark, S. C. Wilks, N. Meezan, R. L. Berger, J. Wurtele, N. J. Fisch, V. M. Malkin, E. J. Valeo, S. F. Martins, and C. Joshi, "Development of a nanosecond-laser-pumped Raman amplifier for short laser pulses in plasma," Phys. Plasmas **16**, 123113 (2009).

[16]R. M. G. M. Trines, F. Fiúza, R. Bingham, R. A. Fonseca, L. O. Silva, R. A. Cairns, and P. A. Norreys, "Simulations of efficient Raman amplification into the multipetawatt regime," Nat. Phys. **7**, 87–92 (2011).

[17]G. Vieux, A. Lyachev, X. Yang, B. Ersfeld, J. Farmer, E. Brunetti, R. Issac, G. Raj, G. Welsh, S. Wiggins, *et al.*, "Chirped pulse Raman amplification in plasma," New J. Phys. **13**, 063042 (2011).

[18]N. A. Yampolsky and N. J. Fisch, "Limiting effects on laser compression by resonant backward Raman scattering in modern experiments," Phys. Plasmas **18**, 056711 (2011).

[19]G. Vieux, S. Cipiccia, D. W. Grant, N. Lemos, P. Grant, C. Ciocarlan, B. Ersfeld, M. S. Hur, P. Lepipas, G. G. Manahan, G. Raj, D. Reboredo Gil, A. Subiel, G. H. Welsh, S. M. Wiggins, S. R. Yoffe, J. P. Farmer, C. Aniculaesei, E. Brunetti, X. Yang, R. Heathcote, G. Nersisyan, C. L. S. Lewis, A. Pukhov, J. M. Dias, and D. A. Jaroszynski, "An ultra-high gain and efficient amplifier based on Raman amplification in plasma," Sci. Rep. **7**, 2399 (2017).

[20]D. Turnbull, S. Bucht, A. Davies, D. Haberberger, T. Kessler, J. L. Shaw, and D. H. Froula, "Raman amplification with a flying focus," Phys. Rev. Lett. **120**, 024801 (2018).

[21]A. A. Balakin, D. S. Levin, and S. A. Skobelev, "Compression of laser pulses due to Raman amplification of plasma noises," Phys. Rev. A **102**, 013516 (2020).

[22]A. Andreev, C. Riconda, V. Tikhonchuk, and S. Weber, "Short light pulse amplification and compression by stimulated Brillouin scattering in plasmas in the strong coupling regime," Phys. Plasmas **13**, 053110 (2006).

[23]L. Lancia, J.-R. Marquès, M. Nakatsutsumi, C. Riconda, S. Weber, S. Hüller, A. Mančić, P. Antici, V. T. Tikhonchuk, A. Héron, P. Audebert, and J. Fuchs, "Experimental evidence of short light pulse amplification using strong-coupling stimulated Brillouin scattering in the pump depletion regime," Phys. Rev. Lett. **104**, 025001 (2010).

[24]G. Lehmann and K. H. Spatschek, "Nonlinear Brillouin amplification of finite-duration seeds in the strong coupling regime," Phys. Plasmas **20**, 073112 (2013).

[25]C. Riconda, S. Weber, L. Lancia, J.-R. Marquès, G. A. Mourou, and J. Fuchs, "Spectral characteristics of ultra-short laser pulses in plasma amplifiers," Phys. Plasmas **20**, 083115 (2013).

[26]M. R. Edwards, J. M. Mikhailova, and N. J. Fisch, "X-ray amplification by stimulated Brillouin scattering," Phys. Rev. E **96**, 023209 (2017).

[27]R. K. Kirkwood, D. P. Turnbull, T. Chapman, S. C. Wilks, M. D. Rosen, R. A. London, L. A. Pickworth, W. H. Dunlop, J. D. Moody, D. J. Strozzi, P. A. Michel, L. Divol, O. L. Landen, B. J. MacGowan, B. M. Van Wonterghem, K. B. Fournier, and B. E. Blue, "Plasma-based beam combiner for very high fluence and energy," Nat. Phys. **14**, 80–84 (2018).

[28]Y. Shi, H. Qin, and N. J. Fisch, "Laser-plasma interactions in magnetized environment," Phys. Plasmas **25**, 055706 (2018).

[29]M. R. Edwards, Y. Shi, J. M. Mikhailova, and N. J. Fisch, "Laser amplification in strongly magnetized plasma," Phys. Rev. Lett. **123**, 025001 (2019).

[30]M. H. Muendel and P. L. Hagelstein, "Four-wave frequency conversion of coherent soft x rays in a plasma," Phys. Rev. A **44**, 7573–7579 (1991).

[31]S. Tang, Y. Yin, C. Xiao, H. Zhuo, T. Yu, D. Zou, and F. Shao, "Laser amplification by four-wave mixing in plasmas," in *Fifth International Symposium on Laser Interaction with Matter* (International Society for Optics and Photonics, 2019), Vol. 11046, p. 110460Z.

[32]V. M. Malkin and N. J. Fisch, "Towards megajoule x-ray lasers via relativistic four-photon cascade in plasma," Phys. Rev. E **101**, 023211 (2020).

[33]V. M. Malkin and N. J. Fisch, "Resonant four-photon scattering of collinear laser pulses in plasma," Phys. Rev. E **102**, 063207 (2020).

[34]K. J. Burns, G. M. Vasil, J. S. Oishi, D. Lecoanet, and B. P. Brown, "Dedalus: A flexible framework for numerical simulations with spectral methods," Phys. Rev. Res. **2**, 023068 (2020).